TWELFTH EUROPEAN ROTORCRAFT FORUM

Paper No. 49

AN ADVANCED MATHEMATICAL MODEL FOR HELICOPTER
FLIGHT SIMULATION USING NONLINEAR UNSTEADY AERODYNAMICS

Ulrich Leiss
Siegfried Wagner

Universität der Bundeswehr
Institut für Luftfahrttechnik und Leichtbau
München, F.R. Germany

September 22 - 25, 1986

Garmisch-Partenkirchen

Federal Republic of Germany

AN ADVANCED MATHEMATICAL MODEL FOR HELICOPTER FLIGHT SIMULATION USING NONLINEAR UNSTEADY AERODYNAMICS

Ulrich Leiss
Siegfried Wagner

Universität der Bundeswehr
Institut für Luftfahrttechnik und Leichtbau
München, F.R. Germany

Abstract:

The dynamic behaviour of helicopters is often represented by a highly so-
phisticated theoretical dynamic model but uses aerodynamics that are not ad-
equate. Modern helicopter simulation programs use blade element rotor model-
ling with aerodynamic data from tables.
Therefore, a new mathematical model was formulated for application to a wide
variety of helicopter configurations. Quaternions and Euler transformations
describe the extended degrees of freedom.
A new generalized aerodynamic model is the key for the manifold progress.
Aerodynamic coefficients were expressed in analytical form. Thus, blade ele-
ments were eliminated by analytical integration in radial direction. A new
approach to inflow and threedimensional effects was included. Viscous and
nonviscous unsteady effects were formulated separately for pitch, plunge,
yaw and fore and aft motion. Separated and reverse flow can be evaluated at
high advance ratios and heavily loaded rotors.
The application of the new model leads to improved numerical stability and
accuracy. Computation time decreases significantly. New effects can be ana-
lysed at isolated rotors or complete helicopters in future.

1. Introduction

The need of increased performance, improved handling qualities and extended
flight envelope leads to the investigation of new evolutionary and revoluti-
onary rotary wing aircraft concepts. Design is often close to physical li-
mits and therefore a powerful tool is required to develop new helicopters.
Due to the fast progress of computers simulation capabilities have improved
significantly in the last few years. On this basis simulation is utilized
for a wide variety of applications (1,2). Whether computer simulation, ground
based aircraft simulation or inflight simulation is used, the principal item
of simulation is the mathematical model.
Because of the complexity and cost of such an analysis and computer program,
work is concentrated on the formulation of universally applicable simulation
models (3,4,5). The dynamic behaviour is represented by increasing degrees
of freedom but the aerodynamic contribution is interpolated from table look-
ups. Therefore, the main objectives of the present investigation is the re-
formulation of rotor blade aerodynamics.
First of all, the chosen rotary wing aircraft dynamics model consists of a
6 DOF rigid body and n arbitrary oriented 3 DOF rotors. Every rotor can have
one or more 3 DOF rigid blade segments. Coupling of all degrees of freedom
is fundamentally possible. The number of necessary transformations leads to
a unified rotational degree of freedom formulation with Quaternions inclu-
ding arbitrary angles without singularities. The Euler transformation matrix

of the blade segments was developed into a power series expansion to avoid trigonometric functions in the whole dynamics model. The number of expansion elements was selected on the finite error assumption of subsequent blade segment transformations. Differential equations were formulated according to the maximum DOF version of the dynamics model.

The second and key part of the general mathematical model is the analytical nonlinear steady and unsteady aerodynamic model. An adequate modelling of dynamic and aerodynamic forces and moments is required. For consistency the classical aerodynamic polar coordinates were replaced by a blade fixed cartesian system. Aerodynamic coefficients were expressed directly on velocity and acceleration components in the new coordinate system. The superposition of different flow types enables a continuous analytical description of steady and unsteady, nonviscous and viscous aerodynamic effects. A new threedimensional rotor blade approach was used to eliminate blade elements. The modular aerodynamic structure consists of the isolated contribution of fuselage, wings and rotors and a generalized interference effect matrix.

For the sake of completeness the engine and control model is necessary but beyond the scope of the present investigation. Finally some advantages of the applied model are presented, concerning trim convergency, integration and computation time.

2. Dynamic Model

2.1 Coordinate Systems

A modular structure demands separate coordinates for any subsystem. The arrangement of coordinates is shown in Fig. 1 for a standard helicopter.

S   CENTER OF GRAVITY

F   FUSELAGE

W_i WINGS

Ro_i ROTORS
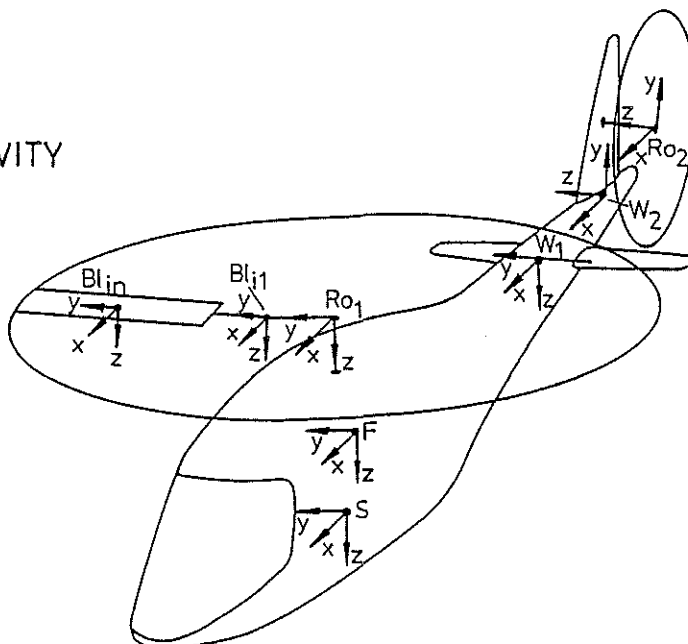
Bl_{ii} ROTOR BLADES

Fig. 1 Coordinate systems of the helicopter

Different systems for the center of gravity and fuselage are comfortable when S moves. The so called wing system was used for horizontal and vertical stabilizers or other lifting surfaces. One rotating system is needed for the center of gravity of any rotor. One or more coordinate systems describe the real or equivalent blade hinges.

2.2 Euler Transformations

To generalize the model all rotational degrees of freedom were formulated with Euler angles. The definition of axes and angles in the fuselage center of gravity system is shown in Fig.2.
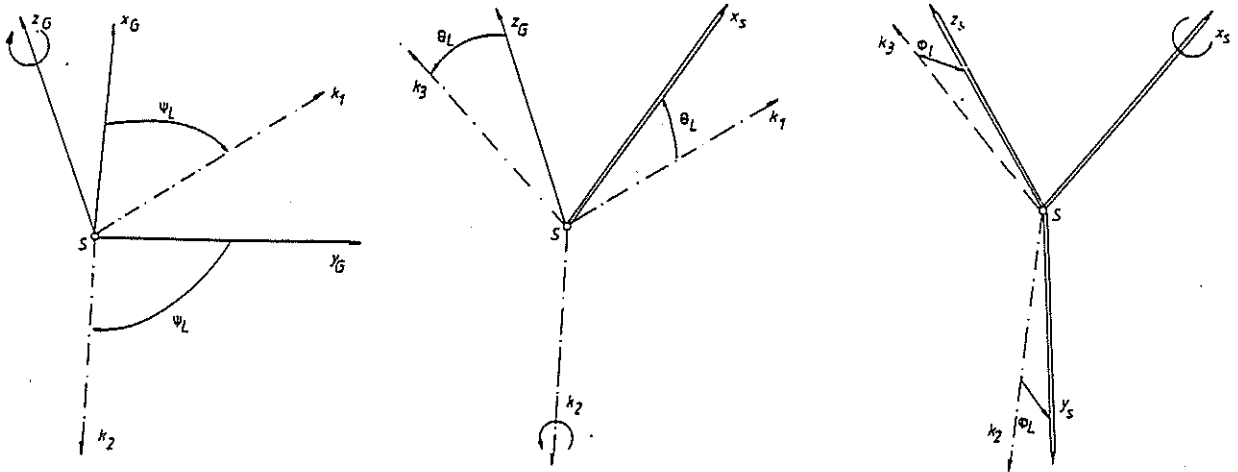
Fig.2 Euler Transformation x - sequence, C.G. Fuselage

The corresponding matrices were:

$$
\begin{bmatrix}
1 & 0 & 0 \\
0 & \cos\phi_L & \sin\phi_L \\
0 & -\sin\phi_L & \cos\phi_L
\end{bmatrix}
\begin{bmatrix}
\cos\theta_L & 0 & -\sin\theta_L \\
0 & 1 & 0 \\
\sin\theta_L & 0 & \cos\theta_L
\end{bmatrix}
\begin{bmatrix}
\cos\psi_L & \sin\psi_L & 0 \\
-\sin\psi_L & \cos\psi_L & 0 \\
0 & 0 & 1
\end{bmatrix}
$$

Rotors of modern rotorcraft can be oriented in any spatial direction. The corresponding unified formulation is a z - sequence Euler angle rotation as shown in Fig.3.
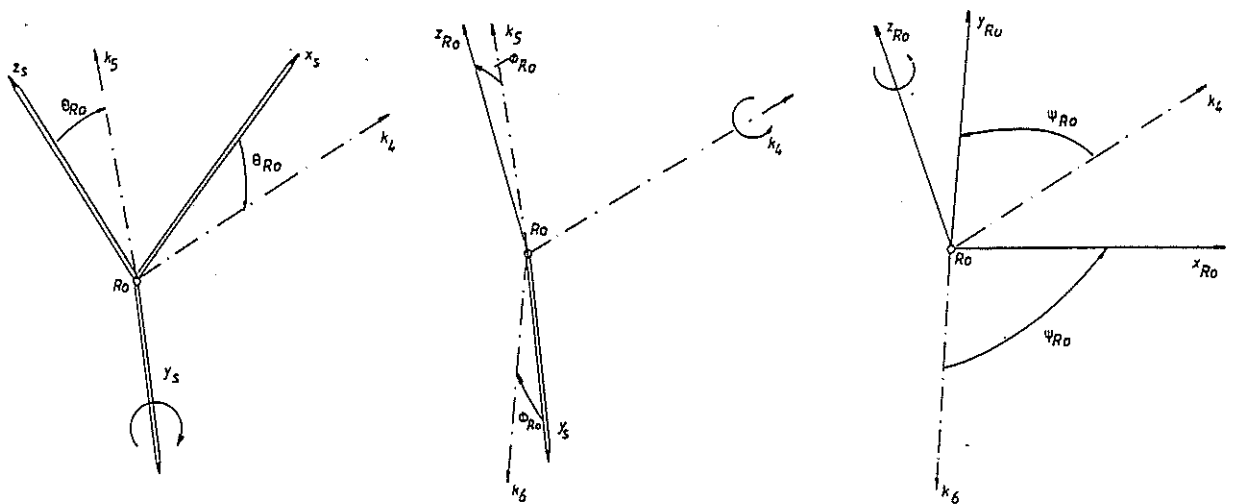
Fig.3 Euler Transformation z - sequence, Rotor Hub

The corresponding matrices were:

$$\begin{bmatrix} \cos\Psi_{RO} & \sin\Psi_{RO} & 0 \\ -\sin\Psi_{RO} & \cos\Psi_{RO} & 0 \\ 0 & 0 & 1 \end{bmatrix} \begin{bmatrix} 1 & 0 & 0 \\ 0 & \cos\Phi_{RO} & \sin\Phi_{RO} \\ 0 & -\sin\Phi_{RO} & \cos\Phi_{RO} \end{bmatrix} \begin{bmatrix} \cos\theta_{RO} & 0 & -\sin\theta_{RO} \\ 0 & 1 & 0 \\ \sin\theta_{RO} & 0 & \cos\theta_{RO} \end{bmatrix}$$

Finally the blade motion was modelled by one ore more spherical joints. So the arrangement of real or effective hinges can be changed without reformulating the model. One system is normally sufficient for the purpose of flight simulation. The used x – sequence is the same as for the rigid body. (Fig.4)
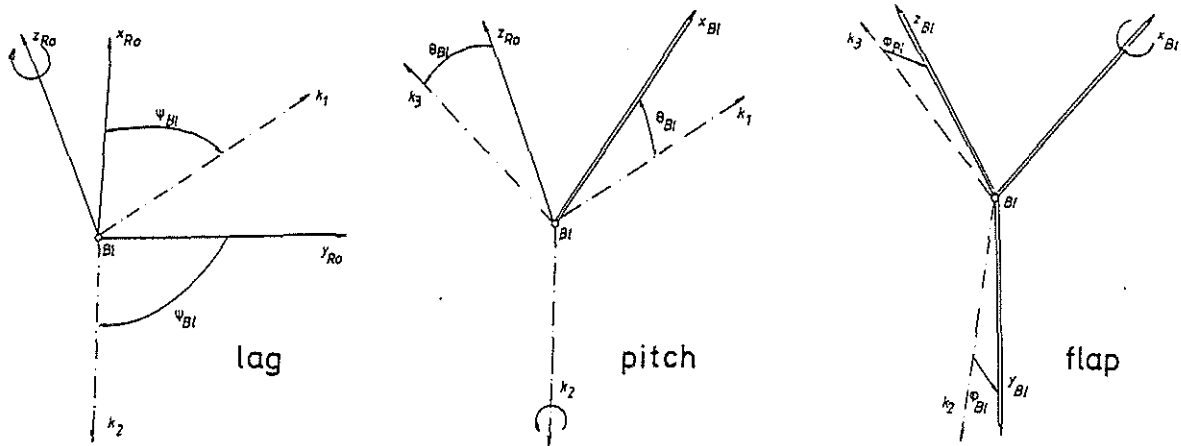

Fig.4 Euler Transformation x – sequence, Rotor Blade

The difference is a small angle formulation of the transformation matrix as follows:

$$\begin{bmatrix} 1 - \frac{1}{2}(\Psi_{BL1}^2 + \Theta_{BL1}^2) & \Psi_{BL1} - \frac{1}{2}\Psi_{BL1}\Theta_{BL1}^2 - \frac{1}{6}\Psi_{BL1}^3 & -\Theta_{BL1} + \frac{1}{6}\Theta_{BL1}^3 \\[2ex] \begin{aligned} &-\Psi_{BL1} + \Theta_{BL1}\Phi_{BL1} + \frac{1}{2}\Psi_{BL1}\Phi_{BL1}^2 + \frac{1}{6}\Psi_{BL1}^3 \\ &-\frac{1}{6}(\Theta_{BL1}^3\Phi_{BL1} + \Theta_{BL1}\Phi_{BL1}^3) - \frac{1}{2}\Psi_{BL1}^2\Theta_{BL1}\Phi_{BL1} \end{aligned} & 1 - \frac{1}{2}(\Psi_{BL1}^2 + \Phi_{BL1}^2) + \Psi_{BL1}\Theta_{BL1}\Phi_{BL1} & \Phi_{BL1} - \frac{1}{2}\Theta_{BL1}^2\Phi_{BL1} - \frac{1}{6}\Phi_{BL1}^3 \\[2ex] \begin{aligned} &\Theta_{BL1} + \Psi_{BL1}\Phi_{BL1} \\ &-\frac{1}{2}(\Theta_{BL1}\Phi_{BL1}^2 + \Psi_{BL1}^2\Theta_{BL1}) - \frac{1}{6}\Theta_{BL1}^3 \end{aligned} & \begin{aligned} &-\Phi_{BL1} + \Psi_{BL1}\Theta_{BL1}\Phi_{BL1} + \frac{1}{2}\Psi_{BL1}^2\Phi_{BL1} + \frac{1}{6}\Phi_{BL1}^3 \\ &-\frac{1}{6}(\Psi_{BL1}\Theta_{BL1}^2 + \Psi_{BL1}^3\Theta_{BL1}) - \frac{1}{2}\Psi_{BL1}\Theta_{BL1}\Phi_{BL1}^2 \end{aligned} & 1 - \frac{1}{2}(\Theta_{BL1}^2 + \Phi_{BL1}^2) \end{bmatrix}$$

The selection of expansion elements was due to a finite maximum error for subsequent blade system transformations in comparison with the exact formulation. On this basis the multiple blade transformation is reduced to an element summation.

2.3 Fuselage Degrees Of Freedom

The fuselage is modelled with a 6 DOF rigid body as usual in practise for fixed wing aircraft. Fig.5 illustrates the orientation of the six state variables in the center of gravity system.
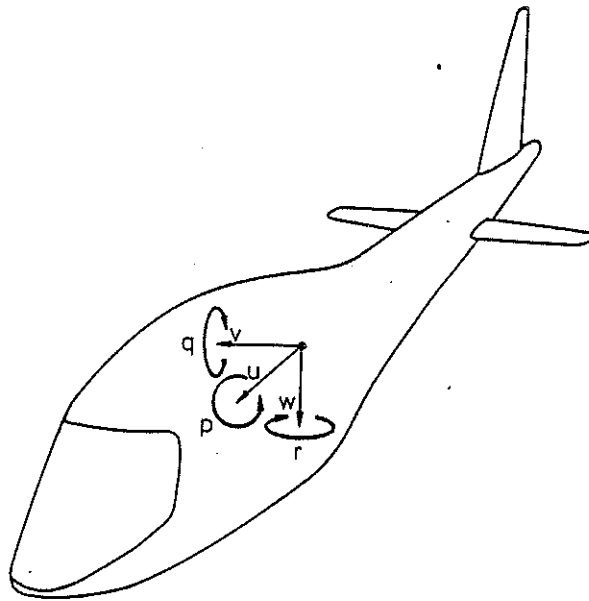

Fig.5 Fuselage Degrees Of Freedom

The differential equations of motion according to an arbitrary nonsymmetric body are:

Translatory:

$$\left(\begin{bmatrix} \dot{u} \\ \dot{v} \\ \dot{w} \end{bmatrix} + \begin{bmatrix} u \\ v \\ w \end{bmatrix} \times \begin{bmatrix} p \\ q \\ r \end{bmatrix} \right) \cdot m = \overline{F}$$

Rotatory:

$$\begin{bmatrix} \dot{p} \\ \dot{q} \\ \dot{r} \end{bmatrix} \cdot \overline{\overline{I}} + \begin{bmatrix} p \\ q \\ r \end{bmatrix} \times \begin{bmatrix} p \\ q \\ r \end{bmatrix} \cdot \overline{\overline{I}} = \overline{M}$$

2.4 Rotor Degrees Of Freedom

For the purpose of modelling tilt rotors, moveable aftbody fans or the effect of shaft bending the full system of rotational differential equations of motion is given by:

$$\begin{bmatrix} \dot{p}_{Ro} \\ \dot{q}_{Ro} \\ \dot{r}_{Ro} \end{bmatrix} \cdot \overline{\overline{I}}_{Ro} + \begin{bmatrix} p_{Ro} \\ q_{Ro} \\ r_{Ro} \end{bmatrix} \times \begin{bmatrix} p_{Ro} \\ q_{Ro} \\ r_{Ro} \end{bmatrix} \cdot \overline{\overline{I}}_{Ro} = \overline{M}_{Ro}$$

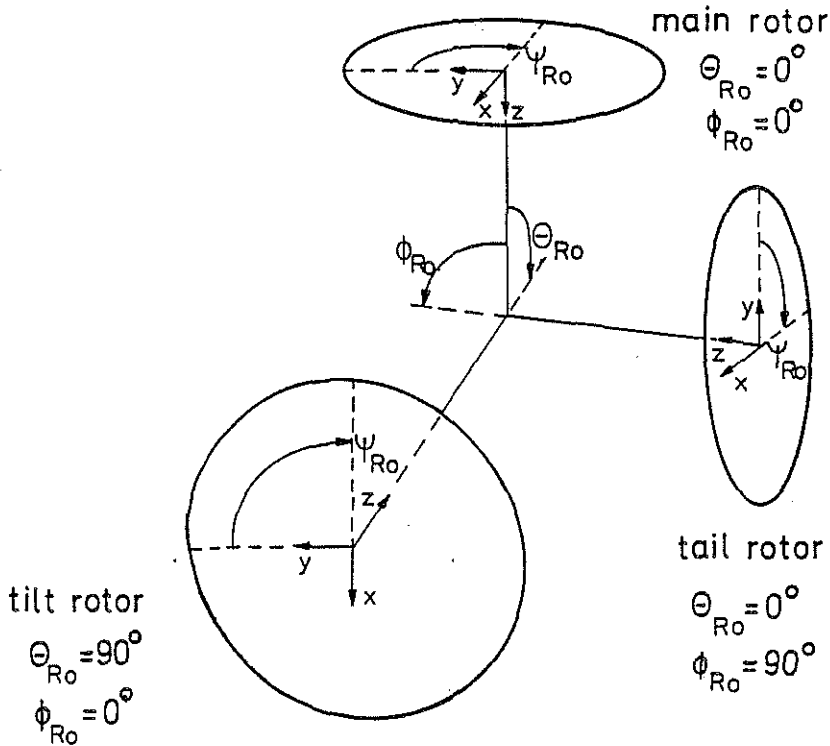The typical rotor positions are illustrated in Fig.6.

Fig.6 Rotor Degrees Of Freedom

One major difference from other models arises at the zero degree azimuth position. But saving the intermediate frame gives some advantages in combination with the reformulated aerodynamic model.

2.5 Quaternion Transformations

Quaternions are hypercomplex numbers and have been introduced to flight mechanics since a longer time (6,7). The equivalence between Quaternions and Euler angles is given as follows:
x − sequence:

$$\Lambda_0 = \cos\frac{\Phi_L}{2}\cos\frac{\Psi_L}{2}\cos\frac{\theta_L}{2} + \sin\frac{\Phi_L}{2}\sin\frac{\theta_L}{2}\sin\frac{\Psi_L}{2}$$

$$\Lambda_1 = \sin\frac{\theta_L}{2}\cos\frac{\Phi_L}{2}\sin\frac{\Psi_L}{2} - \sin\frac{\Phi_L}{2}\cos\frac{\theta_L}{2}\cos\frac{\Psi_L}{2}$$

$$\Lambda_2 = -\sin\frac{\theta_L}{2}\cos\frac{\Phi_L}{2}\cos\frac{\Psi_L}{2} - \sin\frac{\Phi_L}{2}\cos\frac{\theta_L}{2}\sin\frac{\Psi_L}{2}$$

$$\Lambda_3 = -\cos\frac{\Phi_L}{2}\cos\frac{\theta_L}{2}\sin\frac{\Psi_L}{2} + \sin\frac{\Phi_L}{2}\sin\frac{\theta_L}{2}\cos\frac{\Psi_L}{2}$$

z – sequence:

$$\Lambda_0 = \cos\frac{\Psi_{RO}}{2}\cos\frac{\Phi_{RO}}{2}\cos\frac{\Theta_{RO}}{2} + \sin\frac{\Psi_{RO}}{2}\sin\frac{\Phi_{RO}}{2}\sin\frac{\Theta_{RO}}{2}$$

$$\Lambda_1 = -\cos\frac{\Psi_{RO}}{2}\sin\frac{\Phi_{RO}}{2}\cos\frac{\Theta_{RO}}{2} - \sin\frac{\Psi_{RO}}{2}\cos\frac{\Phi_{RO}}{2}\sin\frac{\Theta_{RO}}{2}$$

$$\Lambda_2 = \sin\frac{\Psi_{RO}}{2}\sin\frac{\Phi_{RO}}{2}\cos\frac{\Theta_{RO}}{2} - \cos\frac{\Psi_{RO}}{2}\cos\frac{\Phi_{RO}}{2}\sin\frac{\Theta_{RO}}{2}$$

$$\Lambda_3 = -\sin\frac{\Psi_{RO}}{2}\cos\frac{\Phi_{RO}}{2}\cos\frac{\Theta_{RO}}{2} + \cos\frac{\Psi_{RO}}{2}\sin\frac{\Phi_{RO}}{2}\sin\frac{\Theta_{RO}}{2}$$

Fortunately the corresponding Quaternion transformation matrix is independent of the choice of sequence.

$$\begin{bmatrix} \Lambda_0^2 + \Lambda_1^2 - \Lambda_2^2 - \Lambda_3^2 & 2(\Lambda_1\Lambda_2 - \Lambda_0\Lambda_3) & 2(\Lambda_1\Lambda_3 + \Lambda_0\Lambda_2) \\ 2(\Lambda_1\Lambda_2 + \Lambda_0\Lambda_3) & \Lambda_0^2 - \Lambda_1^2 + \Lambda_2^2 - \Lambda_3^2 & 2(\Lambda_2\Lambda_3 - \Lambda_0\Lambda_1) \\ 2(\Lambda_1\Lambda_3 - \Lambda_0\Lambda_2) & 2(\Lambda_2\Lambda_3 + \Lambda_0\Lambda_1) & \Lambda_0^2 - \Lambda_1^2 - \Lambda_2^2 + \Lambda_3^2 \end{bmatrix}$$

Therefore Quaternions were used simultaneously at the fuselage and the rotor systems. Quaternions avoid singularities and time consuming trigonometric functions. Only one additional variable is necessary.

2.6 Kinematical Differential Equations

Three additional differential equations are required to determine the motion of the rotorcraft.

$$\begin{bmatrix} \dot{\Phi}_L \\ \dot{\Theta}_L \\ \dot{\Psi}_L \end{bmatrix} = \begin{bmatrix} 1 & \dfrac{\sin\Phi_L \, \sin\Theta_L}{\cos\Theta_L} & \dfrac{\cos\Phi_L \, \sin\Theta_L}{\cos\Theta_L} \\ 0 & \cos\Phi_L & -\sin\Phi_L \\ 0 & \dfrac{\sin\Phi_L}{\cos\Theta_L} & \dfrac{\cos\Phi_L}{\cos\Theta_L} \end{bmatrix} \begin{bmatrix} p \\ q \\ r \end{bmatrix}$$

These so-called kinematical equations have singularities when the denominator is zero. The Quaternion formulation offers the following set of four simple differential equations.

$$
\begin{bmatrix} \dot{\Lambda}_0 \\ \dot{\Lambda}_1 \\ \dot{\Lambda}_2 \\ \dot{\Lambda}_3 \end{bmatrix} = \frac{1}{2} \begin{bmatrix} \Lambda_1 & \Lambda_2 & \Lambda_3 \\ -\Lambda_0 & -\Lambda_3 & \Lambda_2 \\ \Lambda_3 & -\Lambda_0 & -\Lambda_1 \\ -\Lambda_2 & \Lambda_1 & -\Lambda_0 \end{bmatrix} \begin{bmatrix} p \\ q \\ r \end{bmatrix}
$$

Once the initial condition is determined by the distinct Euler angles, time dependent Quaternions were evaluated through the above equations.

2.7 Rotor Blade Velocities And Accelerations

Evaluation of the rotor blade local velocities and accelerations is the most elaborative thing in formulating the differential equations of blade motion. First of all the vector from the fuselage center of gravity to any arbitrary blade point is given by the transformation:

$$
\vec{r}_{SP} = \begin{bmatrix} x_{SRO} \\ y_{SRO} \\ z_{SRO} \end{bmatrix} + Q_{RO}^T \begin{bmatrix} x_{BLO} \\ y_{BLO} \\ z_{BLO} \end{bmatrix} + E_1^T \begin{bmatrix} x_{BL1} \\ y_{BL1} \\ z_{BL1} \end{bmatrix}
$$

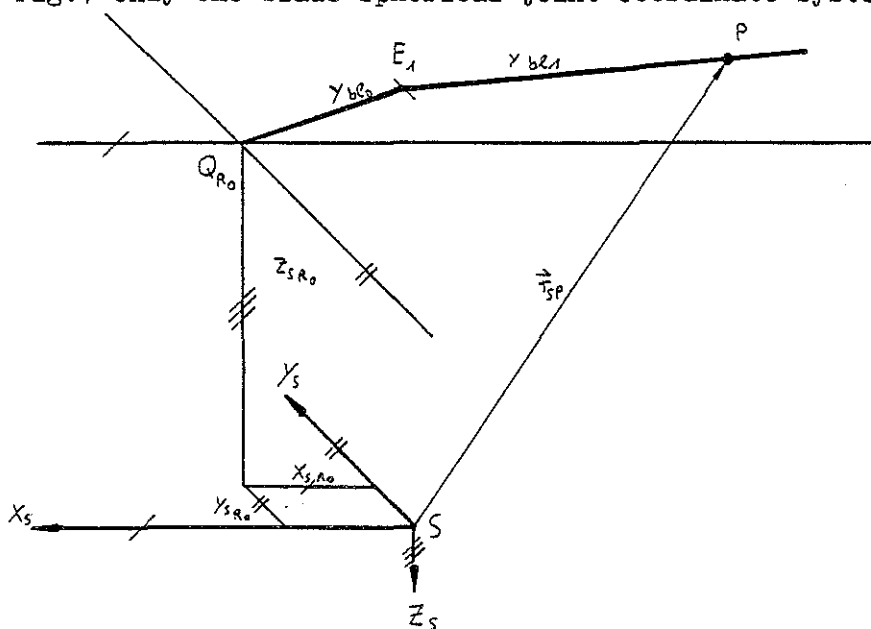As shown in Fig.7 only one blade spherical joint coordinate system was used.

Fig.7 Exemplary coordinate arrangement

For the velocity and acceleration calculation the geodetical contribution must be added.

$$\vec{r}_{GP} = \vec{r}_{GS} + \vec{r}_{SP}$$

Next the absolute velocity and acceleration of a blade point is defined by:

$$\vec{v}_{GP} = \frac{d\,\vec{r}_{GP}}{d\,t} = \frac{d}{d\,t}(\vec{r}_{GS} + \vec{r}_{SP}) = \frac{d\,\vec{r}_{GS}}{d\,t} + \frac{d'\vec{r}_{SP}}{d\,t} + \vec{\Omega} \times \vec{r}_{SP}$$

$$\vec{b}_{GP} = \frac{d^2\vec{r}_{GS}}{d\,t^2} + \frac{d'^2\vec{r}_{SP}}{d\,t^2} + \frac{d\vec{\Omega}}{d\,t} \times \vec{r}_{SP} + \vec{\Omega} \times (\vec{\Omega} \times \vec{r}_{SP}) +$$

$$+ \; 2(\vec{\Omega} \times \frac{d'\vec{r}_{SP}}{d\,t})$$

The evaluation of these equations leds to:

$$\frac{d\,\vec{r}_{GS}}{d\,t} = \vec{v}_{GS} = \begin{bmatrix} u \\ v \\ w \end{bmatrix} \qquad \vec{\Omega} = \begin{bmatrix} p \\ q \\ r \end{bmatrix}$$

$$\vec{r}_{SP} = \begin{bmatrix} x_{SRO} \\ y_{SRO} \\ z_{SRO} \end{bmatrix} + Q_{RO}^T \begin{bmatrix} x_{BLO} \\ y_{BLO} \\ z_{BLO} \end{bmatrix} + Q_{RO}^T E_1^T \begin{bmatrix} x_{BL1} \\ y_{BL1} \\ z_{BL1} \end{bmatrix}$$

$$\dot{\vec{r}}_{SP} = \begin{bmatrix} \dot{x}_{SRO} \\ \dot{y}_{SRO} \\ \dot{z}_{SRO} \end{bmatrix} + (\dot{Q}_{RO}^T E_1^T + Q_{RO}^T \dot{E}_1^T) \begin{bmatrix} x_{BL1} \\ y_{BL1} \\ z_{BL1} \end{bmatrix} + \dot{Q}_{RO}^T \begin{bmatrix} x_{BLO} \\ y_{BLO} \\ z_{BLO} \end{bmatrix}$$

$$\frac{d'^2\vec{r}_{SP}}{d\,t^2} = \begin{bmatrix} \ddot{x}_{SRO} \\ \ddot{y}_{SRO} \\ \ddot{z}_{SRO} \end{bmatrix} + \ddot{Q}_{RO}^T \begin{bmatrix} x_{BLO} \\ y_{BLO} \\ z_{BLO} \end{bmatrix} + (\ddot{Q}_{RO}^T E_1^T + 2\dot{Q}_{RO}^T \dot{E}_1^T + Q_{RO}^T \ddot{E}_1^T) \begin{bmatrix} x_{BL1} \\ y_{BL1} \\ z_{BL1} \end{bmatrix}$$

$$\frac{d^2\,\vec{r}_{GS}}{d\,t^2} = \begin{bmatrix} \dot{u} \\ \dot{v} \\ \dot{w} \end{bmatrix} \qquad \frac{d\vec{\Omega}}{d\,t}\,\vec{r}_{SP} = \begin{bmatrix} \dot{p} \\ \dot{q} \\ \dot{r} \end{bmatrix} \times \begin{bmatrix} r_{SP_x} \\ r_{SP_y} \\ r_{SP_z} \end{bmatrix}$$

$$\vec{\Omega} \times (\vec{\Omega} \times \vec{r}_{SP}) = \begin{bmatrix} p \\ q \\ r \end{bmatrix} \times \left(\begin{bmatrix} p \\ q \\ r \end{bmatrix} \times \begin{bmatrix} r_{SP_x} \\ r_{SP_y} \\ r_{SP_z} \end{bmatrix} \right)$$

$$2(\vec{\Omega} \times \frac{d'\vec{r}_{SP}}{dt}) = 2 \left(\begin{bmatrix} p \\ q \\ r \end{bmatrix} \times \begin{bmatrix} \dot{r}_{SP_x} \\ \dot{r}_{SP_y} \\ \dot{r}_{SP_z} \end{bmatrix} \right)$$

Finally the expression of velocities and accelerations in terms of blade coordinates can be done as follows:

$$\vec{v}_P = E_1 Q_{RO} \vec{v}_{GP} \qquad \vec{b}_P = E_1 Q_{RO} \vec{b}_{GP}$$

Because of the rigid blade model, velocity and acceleration components are linear functions of the corresponding rotor blade coordinates. Therefore the above expressions were reformulated within a long procedure which is not presented here. The resulting coefficients were used simultaneously at the dynamics and aerodynamics model.

2.8 Rotor Blade Inertia Analysis

To obtain the blade differential equations of motion, equilibrium of moments is assumed. Equivalent mechanical systems are composed of spring, damping, inertia and aerodynamic moments.
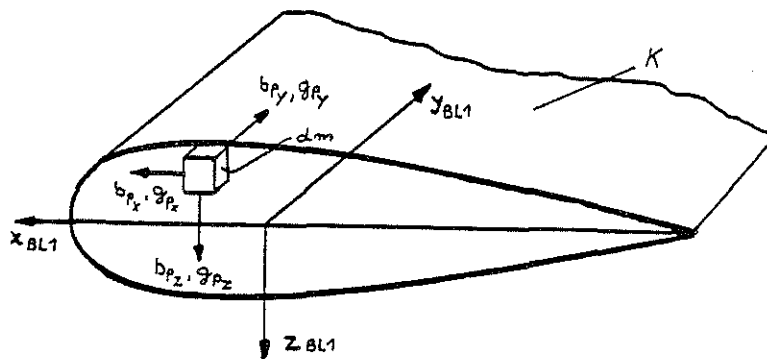Fig.8 shows the differential mass element and the rotor blade axes orientation.

Fig.8 Rotor blade coordinates

The general inertia moments of a rigid blade can be written:

$$M_{M_x} = \int_K \left(\left(-b_{P_z} + g_{P_z}\right) y_{BL1} - \left(-b_{P_y} + g_{P_y}\right) z_{BL1}\right) dm$$

$$M_{M_y} = \int_K \left(\left(-b_{P_x} + g_{P_x}\right) z_{BL1} - \left(-b_{P_z} + g_{P_z}\right) x_{BL1}\right) dm$$

$$M_{M_z} = \int_K \left(\left(-b_{P_y} + g_{P_y}\right) x_{BL1} - \left(-b_{P_x} + g_{P_x}\right) y_{BL1}\right) dm$$

The acceleration due to gravity is obtained by the transformation:

$$\vec{G}_P = \begin{bmatrix} g_{P_x} \\ g_{P_y} \\ g_{P_z} \end{bmatrix} = E_1 Q_{RO} Q_S \begin{bmatrix} 0 \\ 0 \\ g \end{bmatrix}$$

For practical application normally a simplification is introduced like mass concentration. The earlier derived linear acceleration distribution is now appropriate for the analytical evaluation of moments of inertia.

3. Aerodynamic Model

3.1 New Blade Element Definition

As mentioned earlier, great emphasis was given to the improvement and fundamental extension of the state of the art aerodynamic blade modelling for simulation purposes (8,9). The present investigation was carried out for the appropriate combination of the dynamics and the aerodynamics model. In contrast to the common classical aerodynamics, a generalized blade element was formulated as shown in Fig.9.
The classical angle of attack and Mach number dependence of aerodynamic coefficients cannot be linearized without significant loss of accuracy at high angles. The coupling of induced flow or gusts with the freestream results in difficult trigonometric functions.
Therefore the same cartesian coordinate system was used as for the dynamic model. The new blade degrees of freedom are unique. No trigonometric functions occur and the velocity and acceleration components are already available from the inertia analysis. The next problem to solve is now an unified formulation of all aerodynamic coefficients.
First of all the new dimensionless aerodynamic coefficients are expressed as a function of dynamic sonic pressure and Mach number components. Fig.10 illustrates the impact of the coefficient definition.
The new definition has no singularities and represents the real force proportion.

BLADE ELEMENT: classical   new   yaw

angle of
attack   Mach number   fore and aft x pitch   heave
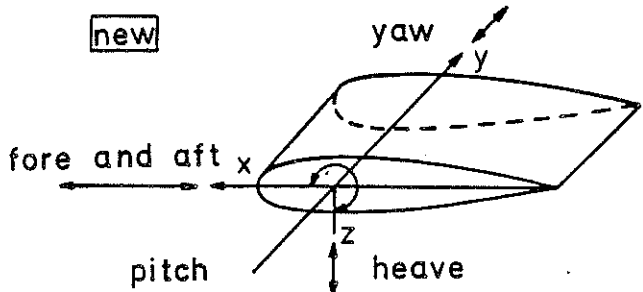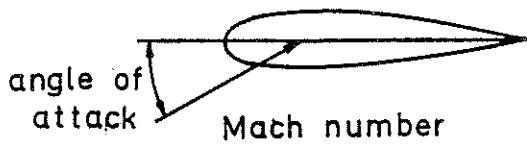
steady : $c_a, c_w, c_m(\alpha, M)$ steady : $c_i(\dot{x}, \dot{y}, \dot{z}, \frac{d\dot{z}}{dx} x)$
yaw correction

aerodynamic coefficients
based on dynamic   unsteady : $c_i(\ddot{x}, \ddot{y}, \ddot{z}, \frac{d\ddot{z}}{dx} x)$
pressure of: similar : $c_i(M_i, Re_i, k_i)$

resultant velocity   speed of sound

Fig.9 Comparison Of Classical And New Blade Element Modelling
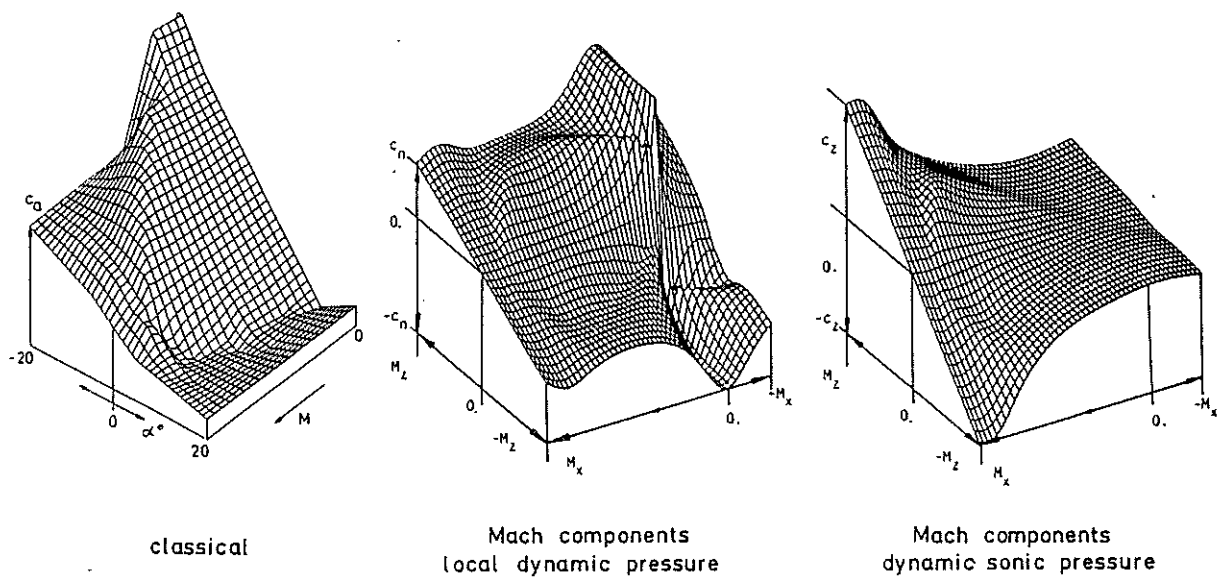
classical   Mach components   Mach components
                             local dynamic pressure   dynamic sonic pressure

Fig.10 Definition Of Aerodynamic Coefficients

3.2 Twodimensional Steady Flow

The necessity to account for the effects of arbitrary oncoming flow directi-
on and similarity parameters led to the superposition of significant flow
types as shown in Fig.11. All flow effects were expressed analytically. The
idealized flow consists of the Newtonian law for all Mach numbers with ad-
ditional circulation corresponding to the fully separated and attached po-
tential flow. Viscosity is responsible for a real behaviour within the range
of the upper and lower potential flow limits. Boundary layer development and
yawed flow triggers trailing and leading edge stall. For completeness super-
sonic theory was applied.

IDEALIZED FLOW

SEPARATED DISPLACEMENT   +   ATTACHED CIRCULATORY   +   SEPARATED CIRCULATORY

BOUNDARY LAYER

TRAILING EDGE STALL   LEADING EDGE STALL

YAWED FLOW
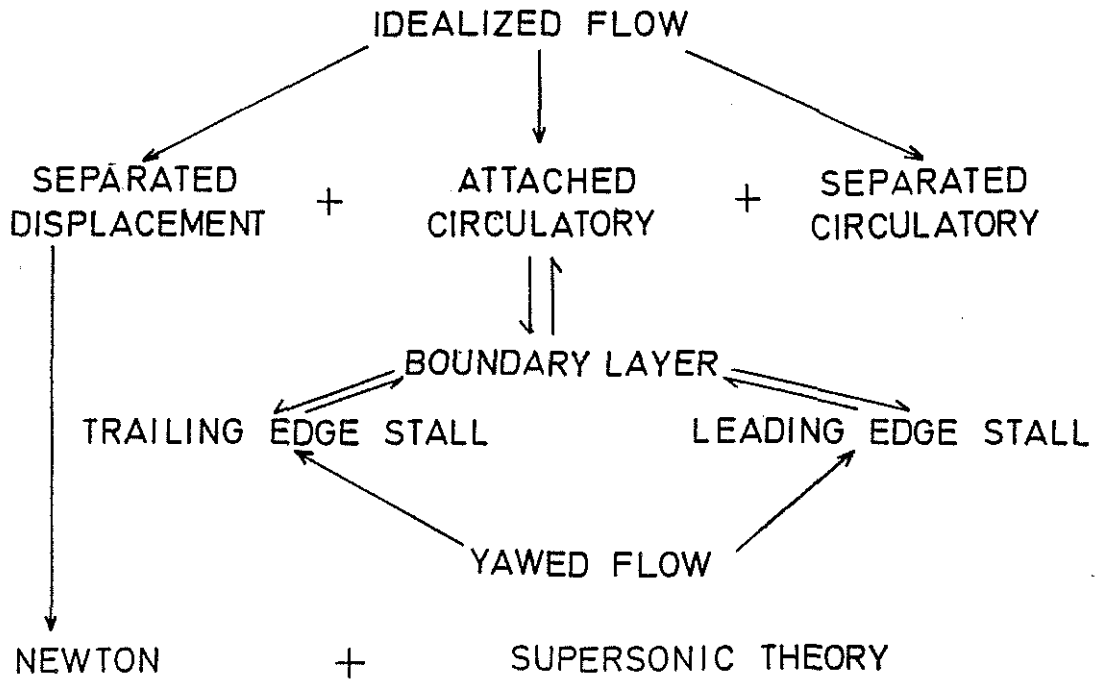
NEWTON   +   SUPERSONIC THEORY

Fig.11 Analytical Model Of Steady Flow

3.3 Twodimensional Unsteady Flow

The unsteady model is based on the steady one and incorporates the time varying effects in the corresponding steady analytical flow subsystems. The structure of unsteady flow is shown in Fig.12.

NONVISCOUS EFFECTS

APPARENT MASS   CIRCULATION LAG   VORTEX PROXIMITY

VISCOUS EFFECTS

BOUNDARY LAYER LAG

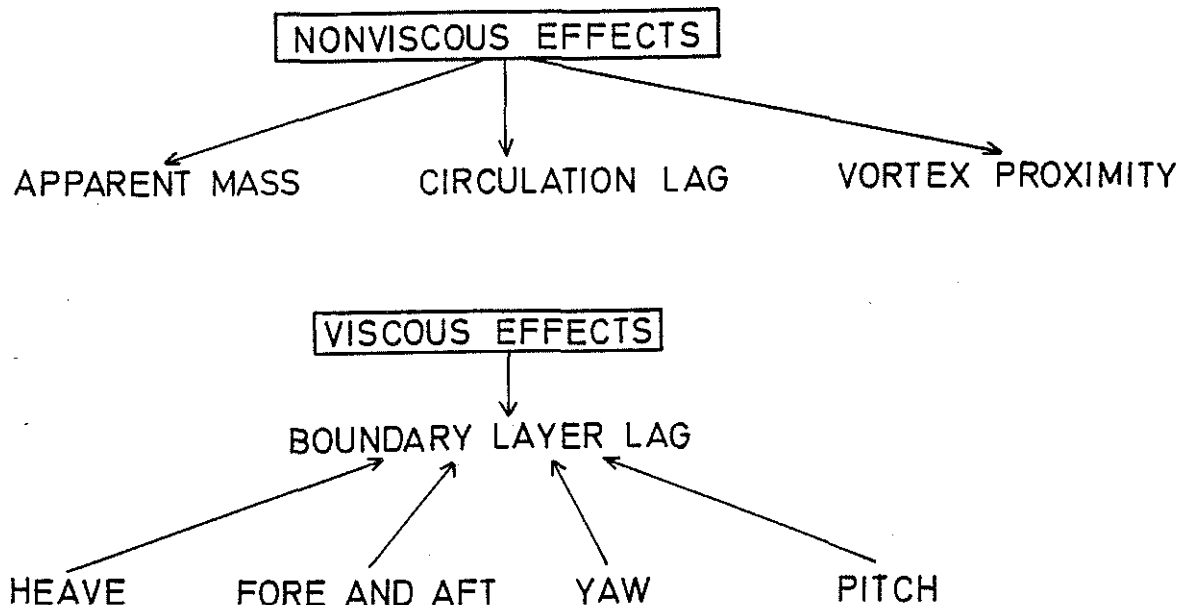HEAVE   FORE AND AFT   YAW   PITCH

Fig.12 Analytical Model Of Unsteady Flow

Now all possible blade degrees of freedom can have important influence on the lag of boundary layer effects. The accuracy of the present steady and unsteady model is compared with measurement in Fig.13.

steady NLR1 —— measurement --- model

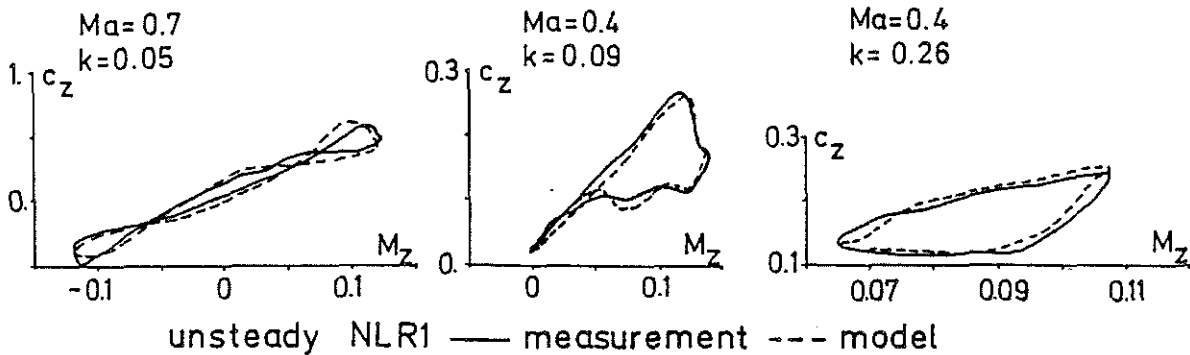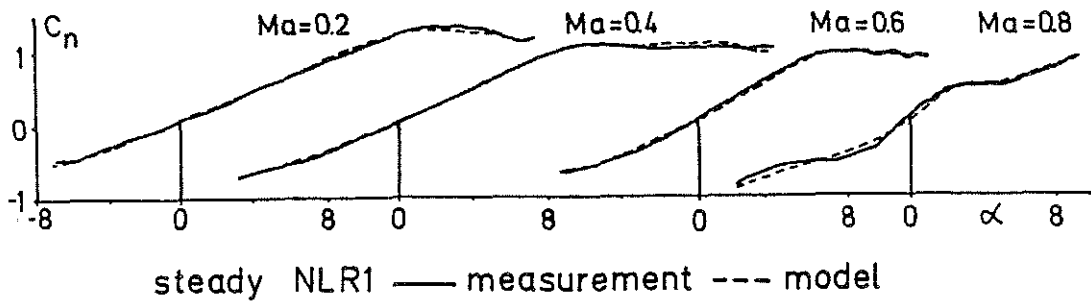unsteady NLR1 —— measurement --- model

Fig.13 Accuracy Of The Analytical Aerodynamic Model

Further basic research work is needed in this field to identify all effects separately and combined.

3.4 Threedimensional Rotor Blade Model

Up to this point all steady and unsteady effects were considered at an element of the infinite rotor blade. At the real rotor blade tip and root the circulation decreases to zero. The common approach to these tip losses is just a reduced blade length. (Fig.14)

classical　　　　　　　　　　　　　　new

integration A - B

analytical load formulation
with near vortex sheet
and continuous tip loss

+momentum theory
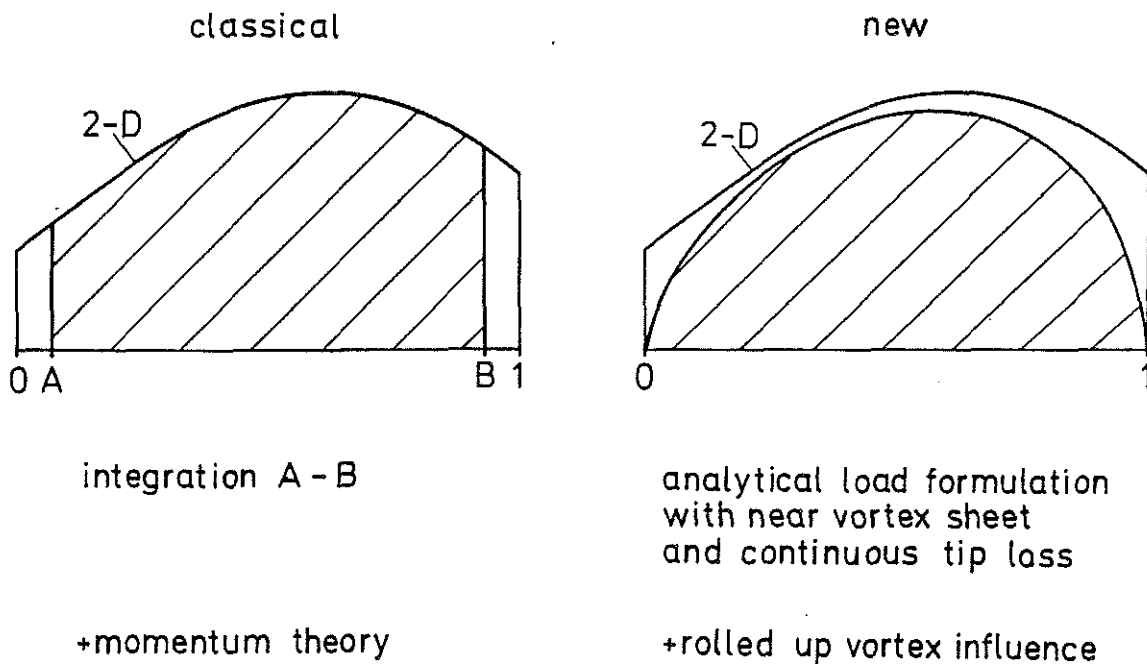
+rolled up vortex influence

Fig.14 Comparison Of 3-D Blade Modelling

The new approach represents the tip loss and the solution of the complex integral equation associated with the vortex induced velocity, by a simple analytical function. Blade elements can be eliminated on this basis and with the present analytical formulation.

3.5 Interaction Of Aerodynamic Subsystems

The aerodynamic coefficient model can be used for all aerodynamic subsystems in a similar way. The superposition of all subsystems is not sufficient for realistic rotorcraft simulation fidelity. Therefore a generalized interference effect matrix was introduced to account for the interacting phenomenas. Fig.15 explains the typical interference elements and the subsystems involved.

MODULE	FUSELAGE	$ROTOR_1$	$\cdots_i$	$ROTOR_n$	$WING_1$	$\cdots_i$	$WING_n$
FUSELAGE					X		
$ROTOR_1$	X	$WAKE_1$		X	X		
$\cdots_i$							
$ROTOR_n$				$WAKE_n$			X
$WING_1$					INDUCED FLOW$_1$		
$\cdots_i$							
$WING_n$							INDUCED FLOW$_n$
GROUND		X					

Fig.15 Generalized Interference Effect Matrix And Typical Elements

4. Computational advantages

The decision behind the choice of an analytical aerodynamic model was not only a physical but a computational one. Fig.16 makes it evident.
The convergency of a trim calculation with the analytical model was significantly better, starting from identical initial conditions.
The saving of computation time depends on the application level of the aerodynamic model. Fig.17 illustrates the acchieved and expected savings. Consequently a much more sophisticated aerodynamic model will be available for real time simulation in future.
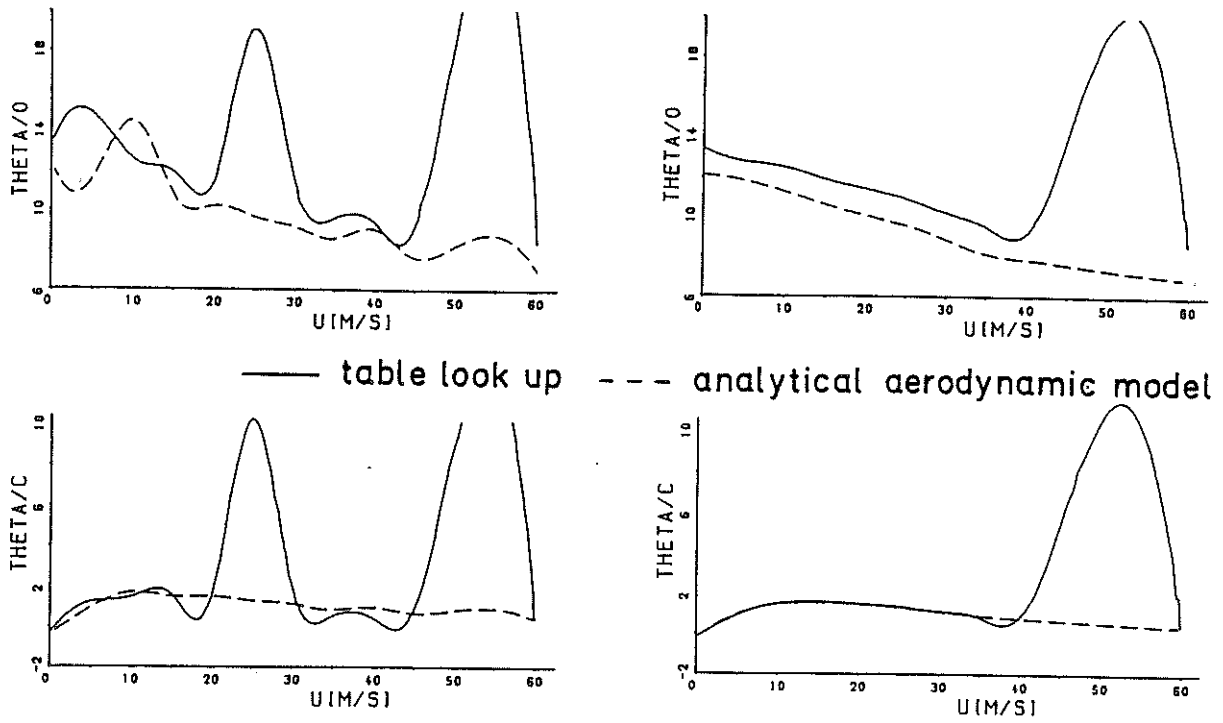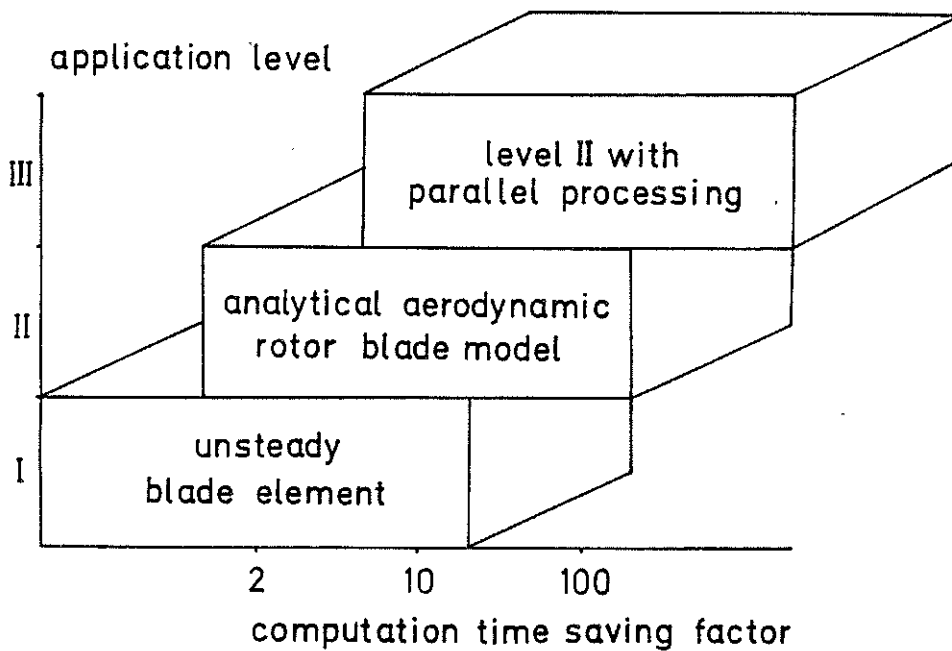
Fig.16 Improved Trim Convergency

Fig.17 Impact Of Analytical Aerodynamic Rotor Blade Modelling

5. Conclusions

An easy to use generalized mathematical model for the purpose of flight mechanics and simulation has been developed. the model was designed to be adequate in dynamics and aerodynamics representation. The simulation capability includes various rotorcraft configurations. Due to the complexity of the investigation only the principle modelling could be presented. The major findings are:
1) The use of Quaternions led to a unique and fast calculation procedure for the fuselage and rotor rotational degrees of freedom.
2) No trigonometric functions occur in the whole model.
3) Inertia and aerodynamic contributions were derived in the same coordinate system.
4) The aerodynamic simulation model is based on the superposition principle and an appropriate interference effect structure.
5) Nonlinear steady and unsteady flow was formulated in analytical form and accounts for arbitrary flow conditions.
6) Unique blade element modelling gives the opportunity to analyze the influence of different blade degrees of freedom on aerodynamics and vice versa.
7) Blade elements were eliminated by a simple 3-D model and subsequent analytical load integration.
8) Numerical stability and trim convergency was improved.
9) Application for real time simulation indicates substantial improvement.
10) Investigations on interference effects are needed.
11) Comparison with flight data is planned for future.

Acknowledgement

References

1) - , Proc. of the international conference on Flight Simulation of Helicopters Status and Prospects, Royal Aeronautical Society, London, 1985

2) H. Huber, P. Krauspe, The Role of Simulation, AGARD Lecture Series No. 139, 1985

3) J.J. Howlett, UH-60A Black Hawk Engineering Simulation Program, United Technologies, Sikorsky Aircraft, Stratford CT (Contract NAS2-10626)

4) W. Johnson, A Comprehensive Analytical Model of Rotorcraft Aerodynamics and Dynamics, NASA TM 81182, 1980

5) D.B. Mackie, T.S. Alderete, A Real Time, Dual Processor Simulation of the Rotor System Research Aircraft, NASA TN D-8328, 1977

6) - , Euler Angles, Quaternions and Transformation Matrices, Working Relationship, Mission Planning and Analysis Division, NASA, July 1977

7) W. Niems, Anwendung der Quaternionen auf die allgemeinen Bewegungsgleichungen der Flugmechanik, ZFW 11, 1963 363-372

8) U. Leiss, A consistent mathematical model to simulate steady and unsteady rotor-blade aerodynamics, Proc. of the 10th European Rotorcraft Forum Paper No.7, The Haag, The Netherlands, 1984

9) U. Leiss, Unsteady sweep a key to simulation of three-dimensional rotor blade airloads, Proc. of the 11th European Rotorcraft Forum Paper No.25 London, England, 1985